UV–visible and fluorescence spectroscopic assessment of meso-tetrakis-(4-halophenyl) porphyrin; H2TXPP (X=F, Cl, Br, I) in THF and THF-water system: Effect of pH and aggregation behaviour

Umar Ali Dar, Shakeel A. Shah

PII: S1386-1425(20)30549-7

DOI: https://doi.org/10.1016/j.saa.2020.118570

Reference: SAA 118570

To appear in: *Spectrochimica Acta Part A: Molecular and Biomolecular Spectroscopy*

Received date: 28 April 2020

Revised date: 28 May 2020

Accepted date: 31 May 2020

Please cite this article as: U.A. Dar and S.A. Shah, UV–visible and fluorescence spectroscopic assessment of meso-tetrakis-(4-halophenyl) porphyrin; H2TXPP (X=F, Cl, Br, I) in THF and THF-water system: Effect of pH and aggregation behaviour, *Spectrochimica Acta Part A: Molecular and Biomolecular Spectroscopy* (2020), https://doi.org/10.1016/j.saa.2020.118570

UV-Visible and Fluorescence Spectroscopic Assessment of Meso-Tetrakis-(4-halophenyl) Porphyrin; H_2TXPP (X=F, Cl, Br, I) in THF and THF-Water System: Effect of pH and Aggregation behaviour

Umar Ali Dar[*, 1], Shakeel A. Shah[**, 1]

[1]*Department of Chemistry, National Institute of Technology Srinagar, Hazratbal, Srinagar-190006, J&K India.*

Abstract

The current study determines optical and fluorescence response of halogen substituted series of meso-tetrakis-(4-halophenyl) porphyrin; H_2TXPP, (Halo= F, Cl, Br, I) dye in tetrahydrofuran; THF and THF-water system at changing pH in relationship with changing medium of allure. Effects produced by varying the pH and medium, over spectral and aggregation were discussed in detail. Results show sequential protonation and deprotonation of H_2TXPP series in acidic (pH = 4) and (pH =10) basic medium. Specific structural changes of monomeric absorption band were put in evidence on lowering pH, which includes broadening and splitting of soret or B band. Other changes include increasing in intensity and red-shifting of Q1 band indicating some degree of aggregation. The side-by- side aggregation and formation of J-aggregate were quite evident. The red shift of B band featured self aggregation through head-to-tail molecular ordering which is consonant with absorption-emission data.

Key words: H_2TXPP, Halogen derivatives, pH sensor, Aggregation

---

*Corresponding author. Department of Chemistry, National Institute of Technology Srinagar, Hazratbal, Srinagar- 190006, J&K India.

**Corresponding author.

E-mail address:drshakeelshah@gmail.com (S.A. Shah),
umar74202@gmail.com (U.A. Dar).

Introduction

Porphyrin compounds are important model systems for chemosensors and photosensitizers [1], widely used in industrial application. Numerous industrial applications such as in the dye [2,3], photography industries [4], and in the new growing fields of molecular electronics [2], photodynamic therapy; (PDT) [5] magnetic resonance imaging; (MRI) [6] and solar energy sensing; (SES) [7] etc . Optical properties and photophysical properties are affected by the presence of substituents at β-pyrrole or at meso-aryl positions of tetraphenylporphyrins; TPP [8–11]. High absorption coefficient and long life time in triplet excited state efficiently produce singlet molecular oxygen [12]. Photophysical properties of porphyrin sensitizers might get affected by change in their aggregation state which could bring changes in absorption spectra [10,13]. Derivatives of substituted porphyrin compounds synthesized are highly sensitive towards electronic absorption spectra on pH variation. The sensitivity is because they have two ionisable protons, Pyrrolic−H on two opposite N−H groups which under goes protonation at around (pH= 4), and deprotonation at (pH= 10). Spectral properties have been monitored by UV-Visible and fluorescence spectroscopy under (a) acidic, (b) basic and neutral condition in aqueous and mixture of aqueous, non-aqueous system. On addition of analyte to the sensitive dye shows significant interference in colour and absorption behaviour. However results displays typical monomeric spectral behaviour in pure organic solvents with typical single soret band and four Q bands of lower intensity [14,15]. Less attention has been received on fluorescent compound which are highly sensitive towards pH variation and particularly for synthetic porphyrin compounds. Porphyrin ring is hydrophobic in nature and highly fluorescent optical pH sensor and could be best alternative for sol-gel silica and polymeric membranes [16]. Due to high immobilization and strong limitation of leaching, this could prove higher potential of covalent immobilization of dye in solid matrix. The urgency and need for monitoring the effect of pH of strongly acidic and basic media, is because they facilitates and responds to various chemical and biological systems such as human body, industrial used waters, acid rain water, medical monitoring [17,18] etc. which involves significant pH changes. Experimental data has proven that medium in the cancerous tissues are acidic, similarly hydrophilic molecules in lysosomes are characteristic of acidic medium [19,20]. Synthetic porphyrin framework with different hetero-atoms at peripheral or at β postion are sensitive sensing compounds for optochemical pH sensors in organic matrix. Therefore it would be worth to explore and could prove effective photosensitizes model compounds of porphyrin in order to understand and tune the chemical recognition and aggregation behaviour. Therefore current study aimed to develop florescent and synthesize chemosensor based on halogen derivative of meso-tetrakis-(4-phenyl) porphyrin; TPP for pH sensing and study their absorption, emission and aggregation behaviour in acidic, basic and neutral medium under THF and THF+ H_2O system.

Experimental

Material and Chemicals

Analytical grade chemicals were used for the synthesis of H_2TXPP. AR grade pyrrole, 4-floro-benzaldehyde, 4-chloro-benzaldehyde, 4-bromobenzaldehyde and 4-iodobenzaldehyde, were purchased from sigma aldrich. However tetrahydrofuran, chloroform and propionic acid, was purchased from Merck and was used as such.

Measurements and Apparatus

FT-IR spectra of these compounds were recorded between 4000 cm^{-1} to 400 cm^{-1} using KBr pellets on Perkin Elmer Spectrum. The elemental analysis was performed on Elementar Vario EL II. ^{1}HNMR of the synthesized compounds was recorded in $CDCl_3$ on Bruker spectrometer, model AV 400 N (400 MHZ) with TMS (tetramethylsilane) used as internal standard. UV-Visible spectra were recorded on Perin Elmier (Lamda 360) spectrophotometer in chloroform; ($CHCl_3$), THF, THF+H_2O system ranging from 200 to 800 nm at different pH variations. However fluorescence spectra were recorded on Shimadzu (RF-5301PC) spectrophotometer in THF and THF+ H_2O system. pH was maintained by hand held digital pH-meter (Cole-parmer, P100)

Spectroscopic studies

Absorption and fluorescence spectra were recorded at room temperature using 1 cm path length cell. To introduce acidic and basic media in analyate solution 0.1 M stock aqueous solution of HCl and NaOH were added and stirred vigorously. The pH was adjusted by digital pH meter. Florescence quantum chemical yield; Φf was calculated by preciously reported equation using TPP area gradient against H_2TXPP [21].

Synthetic procedure used for preparation of H_2TXPP [22–25]

Adler method has been employed using direct condensation reaction of equimolar amounts of freshly distilled pyrrole (20 mmol) and 4-halobenzaldehyde; halo = floro, chloro, bromo and iodo (20 mmol) added to propionic acid (20 ml) and heated to a refluxing temperature.

The solutions were allowed to reflux and put on constant stirring for about 30 minutes. The reaction mixture was allowed to cool at room temperature (30°C). Later reaction mixtures were filtered and the residues were washed with methanol until the filtrates was colourless. The courses of reaction were monitored and purity of these corresponding compounds has been achieved by column chromatography on a basic alumina. However $CHCl_3$ was used as eluent in all cases. Compounds were re-crystallized from $CHCl_3$ on vaccum further subjected to various spectroscopic studies.

H_2TFPP was obtained as shiny purple crystals. Yield 0.46 g (27 %), Anal. data calc. for $C_{44}H_{26}N_4F_4$: C, 76.96; H, 3.82; N, 8.16, found: C, 77.12; H, 3.90; N, 7.96. FT-IR (KBr, cm^{-1}): ν (N-H) 3287, ν (C-H) 3044, ν (C-N) 1378, ν (C=C) 1577, ν (C=N) 1538, (C-H; β-pyrole) 968, ν(C-F) 1199. ^{1}H NMR (400 MHz, $CDCl_3$) δ: 8.84 (s, 8H, porphyrin), 8.17 (d, 8H, Ph), 7.47 (d, 8H, Ph), –2.85 (s, 2H, NH_{imino}). UV-Vis [λmax (nm) in THF/ $CHCl_3$]: 417 (Soret), 514, 549, 590, 649 (Q bands). GC-MS (EI); *m/z*: 687.40 (M^++H).

H_2TClPP was obtained as shiny blue crystals. Yield 0.62 g (41 %). Anal. data calc. for $C_{44}H_{26}N_4Cl_4$: C, 70.23; H, 3.48; N, 7.45, found: C, 71.12; H, 3.09; N, 7.96. FT-IR (KBr, cm^{-1}): ν (N-H) 3317, ν (C-H) 3070, ν (C-N) 1393, ν (C=C) 1589, ν (C=N) 1556, (C-H; β-pyrole) 966, ν(C-Cl) 1089. ^{1}H NMR (400 MHz, $CDCl_3$) δ: 8.86 (s, 8H, Porphyrine), 8.16 (d, 8H, Ph), 7.77 (d, 8H, Ph), –2.84 (s, 2H, NH_{imino}). UV-Vis [λmax (nm) in THF/ $CHCl_3$]: 418 (soret), 514, 550, 590, 646 (Q bands). GC-MS (EI); *m/z*: 753.40 (M^++H).

H_2TBrPP was obtained as shiny blue crystals. Yield 0.62 g (41 %). Anal. data calc. for $C_{44}H_{26}N_4Br_4$: C, 56.81; H, 2.82; N, 6.02, found: C, 56.12; H, 2.60; N, 6.16. FT-IR (KBr, cm^{-1}): ν (N-H) 3312, ν (C-H) 3023, ν (C-N) 1389, ν (C=C) 1586, ν (C=N) 1554, (C-H; β-pyrole) 966, ν(C-Br) 1177. ^{1}H NMR (400 MHz, $CDCl_3$) δ: 8.08 (s, 8H, Porphyrin), 8.26 (d, 8H, Ph), 7.792 (d, 8H, Ph), –2.84 (s, 2H, NH_{imino}). UV-Vis [λmax (nm) in $CHCl_3$]: 418 (soret), 514, 550, 590, 646 (Q bands). GC-MS (EI); *m/z*: 931.20 (M^++H).

H_2TIPP was obtained as shiny dark blue crystals. Yield 0.38 g (21 %). Anal. data calc. for $C_{44}H_{26}N_4I_4$: C, 47.26; H, 2.34; N, 5.01, found: C, 47.23; H, 2.38; N, 5.06. FT-IR (KBr, cm^{-1}): ν (N-H) 3323, ν (C-H) 3084, ν (C-N) 1388, ν (C=C) 1559, ν (C=N) 1539, ν (C-H; β-pyrole) 972, ν(C-I) 1186. ^{1}H NMR (400 MHz, $CDCl_3$) δ: 8.88 (s, 8H, Porphyrin), 8.18 (d, 8H, Ph), 7.86 (d, 8H, Ph), –2.86 (s, 2H, NH_{imino}). UV-Vis [λmax (nm) in $CHCl_3$]: 418 (soret), 514, 550, 590, 646 (Q bands). GC-MS (EI); *m/z*: 1118.82 (M^++H).

Results and discussion

Characterization studies

Synthesized compounds and the reaction scheme employed are shown in Scheme 1. After purification all corresponding compounds were subjected for Elemental analysis, FTIR, GC-MS, ^{1}HNMR. UV-Visible, fluorescence spectroscopy was employed to study the influence of pH and aggregation behaviour on porphyrin derivative in detail.

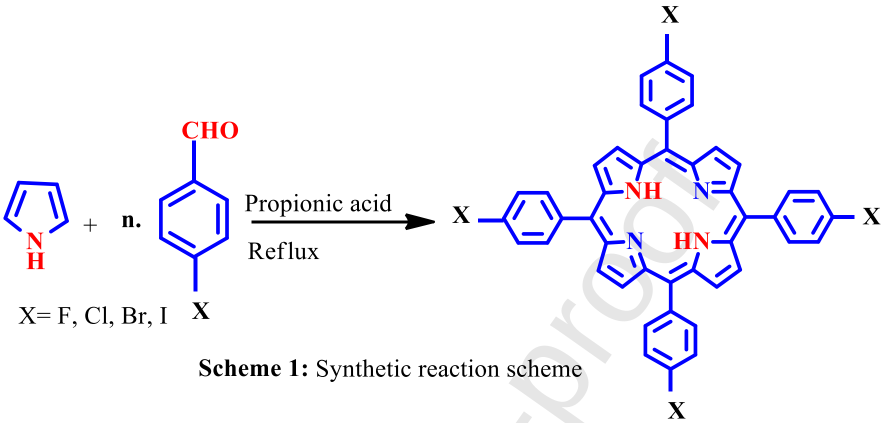

Scheme 1: Synthetic reaction scheme

FT-IR well versed technique to identify the characteristic functional group is presented in Fig. 1 and various frequencies for important functional group are detailed in Table 1. Among all characteristic functional groups, N-H stretching band can be well observed from the spectrum and exhibit N-H stretching vibration at ~3287 cm^{-1} for H_2TFPP, it appears at ~3323 cm^{-1} for H_2TIPP with decreases in frequency by (±5) cm^{-1} for remaining derivatives. A band observed at ~3044 cm^{-1} was attributed to aromatic $\nu_{C\text{-}H}$ stretching frequency for H_2TFPP and 3070 cm^{-1}, 3020 cm^{-1} for Cl and H_2TBrPP. However H_2TIPP appears sharp intense spikes at ~3323 cm^{-1}. ν(C=C/ C=N) appears in the range of ~1589 cm^{-1} to ~1468 cm^{-1}. νC-H (β-pyrole) was assigned ~1330 cm^{-1} with increase in frequency by (±15) cm^{-1} for all other derivatives. The $\nu_{C\text{-}N}$ frequency is observed at ~1330 cm^{-1}, 1344 cm^{-1} and 1346 cm^{-1} for F, Cl, Br and H_2TIPP. The important $\nu_{C\text{-}X}$ was respectively assigned ~1199 cm^{-1} with decreases in frequency by (±15) for remaining derivatives [26,27] . ^{1}HNMR of H_2TXPP series were recorded in $CDCl_3$ to identify characteristic resonating proton analogues of free base porphyrin. All corresponding halo series showed similar pattern with slight or marginal change in chemical shift by (±0.5) ppm. β-pyrole protons and phenyl protons (ortho and meta) resonates in the range of δ = ~7.75-8.55. Most prominent (N−H) proton among all free base porphyrin, which is highly shielded appears at δ= -2.75 as singlet [10,28,29]. UV-visible and emission spectrum was recorded between 200 and 800 nm in pure organic and aqueous electrolyte solution and are discussed in detail in coming section which are in good agreement with literature data [14,15,30].

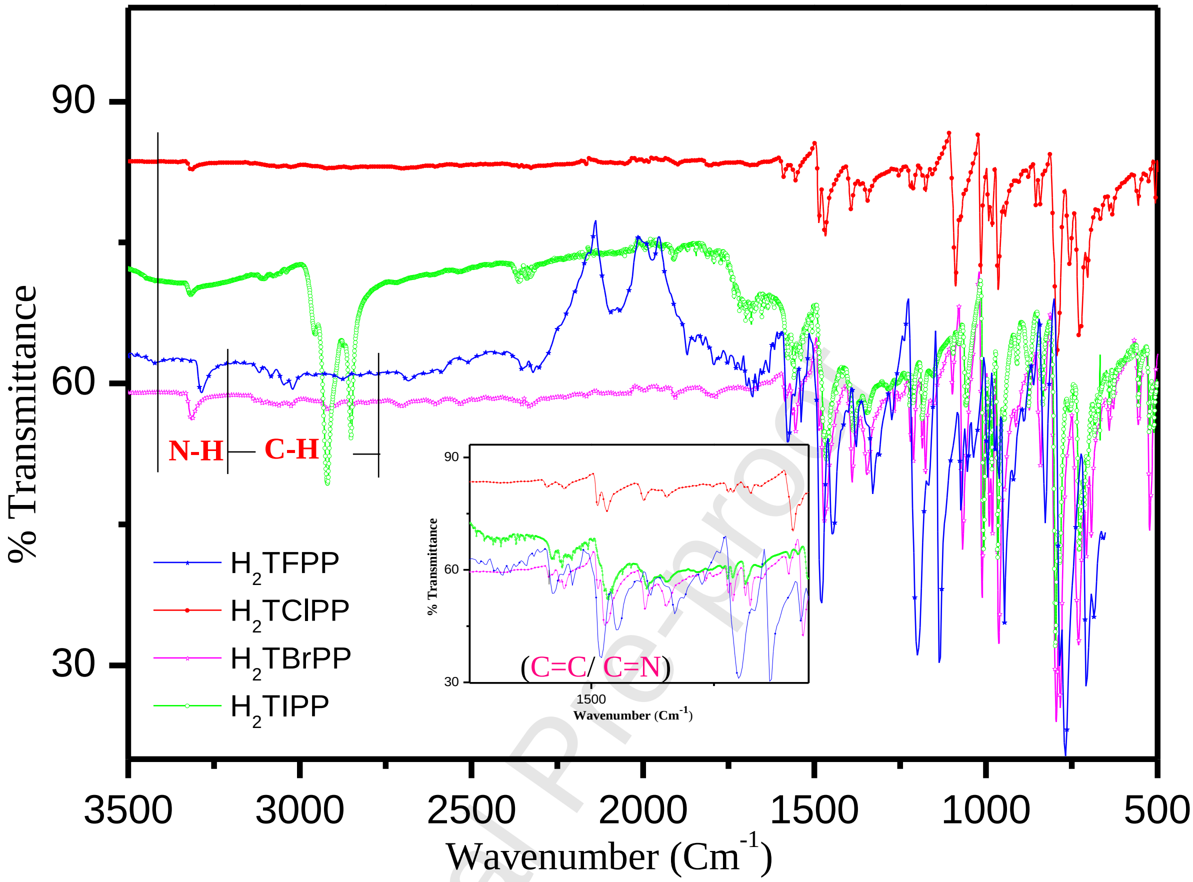

Fig. 1: FT-IR spectrum of H_2TXPP series.

Table 1: Characteristic FT-IR frequencies in cm^{-1} for H_2TXPP series.

R	**H_2TFPP**	**H_2TClPP**	**H_2TBrPP**	**H_2TIPP**
$\nu_{\text{N-H}}$	3287	3317	3312	3323
$\nu_{\text{=C-H (phenyl)}}$	3044	3070	3023	3084
$\nu_{\text{C=C/ C=N}}$	1577, 1538, 1480	1589, 1556, 1468	1586, 1554, 1471	1559, 1539, 1472
$\nu_{\text{C-N}}$	1330	1344	1346	1346
$\nu_{\text{C-H }(\beta\text{-pyrole})}$	968	966	966	972
$\nu_{\text{C-X}}$	1199	1089	1177	1186

Absorption spectroscopy

Porphyrin dye is recognised as essential photosensitizer, highly sensitive towards electronic processes concerning acidic and basic influence [14,31]. Optical absorption and emission spectrum of purified compounds were performed in pure organic solvent i.e. (THF/ $CHCl_3$) for bare halogen derivatives represented in Fig. (2a-2b). The initial pH of halo-derivative in pure solvents was in range of 7-6. However acidic and basic medium was established by addition of aqueous solution of 0.1 M (HCl for Acidic and NaOH for basic) in (1:1, v/v).

THF, water was used because they are highly miscible and form saturated aqueous electrolytic solution. Reports published previously brought acidic and basic medium in $CHCl_3$, which is completely immiscible with aqueous medium. For better optical properties to study, the electrolytic solution must be clear and miscible to overcome inadequate and misleading spectral data. Effect of solvent, variation in polarity and concentration was checked, keeping in view the sensitive structural character of porphyrin, but no significant spectral, either marginal change was observed. Therefore we restricted our observation for pH variation with single solvent of higher solubility concerning halo derivatives. The solubility chart of pure organic solvent in water is represented in Table 2. However the absorption spectra of bare halogen derivatives were recorded between 200 and 800 nm in THF and $CHCl_3$ which displayed two important characteristic bands very important and known among porphyrin compounds. Among these the high intensity band near UV region at λ_{max} ~417 nm originates from Soret or B band for H_2TFPP in both the solvents for Cl, Br, and H_2TIPP it appears at slightly higher wavelength at ~421 nm. Other low intensity band which is further distributed among four weaker bands originated from Q band represented as Q1-Q4. B band are ascribed to π-π* ($a_{1u} \rightarrow e_g$*) electronic transition and arises from ground state (S_0) to second existed state (S_2), when compared with the unsubstituted TPP or TTP. The band shifts toward lower wavelength for floro derivative as expected by (±4) nm because of –I effect exerted by fluorine, suggesting poor π conjugation. However later shifted toward higher wavelength by ~(±4) nm, which is due to increased π conjugation and decrease in HOMO-LUMO energy gap exerted by the electron releasing halogen functional. Indeed Q bands appears in the visible range at λ ~480-650 nm with lower intensity consistent with π-π* ($a_{2u} \rightarrow e_g$) transition from ground state (S_0) to singlet excited state (S_1). Beside above two prominent (B and Q) bands an additional low intensity band appears as shoulder to soret band at around ~365 (±5) nm is assigned to charge transfer transition from lone pair P orbital of peripheral halogen to empty π* orbital for H_2TFPP and H_2TClPP. However for bromo and iodo the charge transfer would be either from n→π*, d→π*, or π→d transitions at higher ionic strength, that appears blue shifted by (±4) nm [10]. and Detailed absorption bands with intensity in parenthesis are presented in Table 3. Overall it was argued and observed that there was marginal or no appreciable change in intensity and position of the characteristic bands on variable solvation.

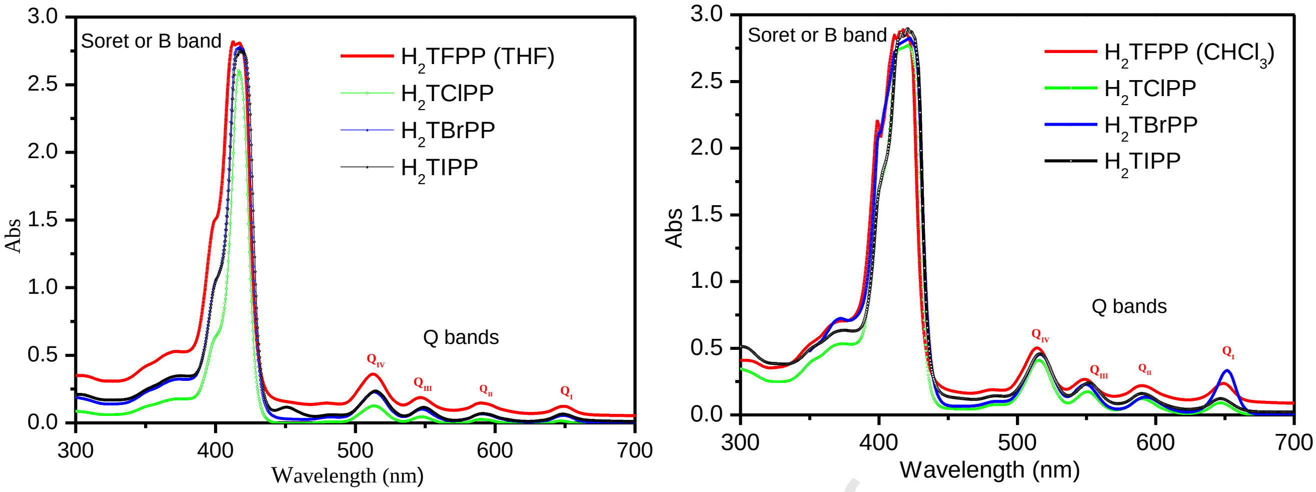

(a) **(b)**

Fig. 2: (**a**) UV-Visible absorption spectrum of monomer in THF, (**b**) $CHCl_3$ at pH=7 (C_M = 3.0×10^{5}M)

Table 2: Solubility chart of H_2TXPP series in various solvents and their nature in H_2O.

H_2TXPP	**$CHCl_3$**	**Acetone**	**MeOH**	**CH_3CN**	**DCM**	**Toluene**	**THF**	**DMSO**
H_2TFPP	partial	partial	insoluble	insoluble	partial	partial	soluble	insoluble
H_2TClPP	soluble	soluble	partial	partial	soluble	partial	soluble	partial
H_2TBrPP	soluble	soluble	partial	partial	soluble	partial	soluble	partial
H_2TIPP	soluble	soluble	partial	partial	soluble	partial	soluble	partial
Water	immiscible	miscible	miscible	miscible	immiscible	immiscible	miscible	miscible

Table 3: Characteristic (Soret or B and Q) bands in nm for H_2TXPP in THF and $CHCl_3$.

THF/ PH=7 (Neutral)	**Sorte or B**			**Q band**		**Ref.**
Sample Codes	**Band**	**QIV**	**QIII**	**QII**	**QI**	
TTP $^{(DCM)}$	420	516	552	592	644	[9]
TPP $^{(THF)}$	419 (3.58)	480 (0.05)	513(0.18)	546(0.08)	648 (0.05)	[15]
TMP $^{(THF)}$	420 (2.95)	516 (0.16)	552 (0.13)	594 (0.06)	651 (0.07)	
H_2TFPP $^{(THF/ CHCl3)}$	417 (2.80)	513 (0.36)	546 (0.18)	589 (0.14)	649 (0.12)	
	417 (2.89)	514 (0.50)	549 (0.26)	590 (0.21)	649 (0.23)	This Work
H_2TClPP	420 (2.60)	513 (0.12)	548 (0.04)	590 (0.02)	646 (0.01)	
	421 (2.77)	515 (0.40)	550 (0.17)	589 (0.12)	646 (0.09)	
H_2TBrPP	421 (2.70)	513 (0.22)	548 (0.10)	590 (0.06)	649 (0.05)	
	422 (2.82)	516 (0.45)	549 (0.22)	592 (0.13)	651 (0.33)	
H_2TIPP	419 (2.70)	514 (0.26)	549 (0.13)	590 (0.08)	647 (0.07)	
	421 (2.89)	516 (0.45)	551 (0.24)	591 (0.16)	647 (0.12)	

Influence of pH

The absorption spectra was recorded under basic (pH=10), and acidic (pH= 5-2) in THF+ H_2O system. The initial colour of H_2TXPP was dark pink and pH was in range of 7-6 at (3.0×10^{5} C_M) i.e. approximately neutral. Upon increasing the acidity by addition of 0.1 M, HCl to the analyate, sudden fascinating colour change was recognized depicted in Fig. 3 with change in absorption spectra. The usual soret band splits into two individual lorentzian bands at ~417 and ~444 nm for floro and 417/ 450, 416/ 448, 417/ 453 nm for Cl, Br and I derivatives consistent with the literature reported [12], [13]. Besides splitting of soret band, the Q bands starts diminishing leaving behind the high intensity Q1 band at ~660 (±10) nm which is otherwise forbidden, accompanied by broadening of soret band at higher ionic strength. This deviation in absorption spectra is attributed to variation in ionic strength developed by the acidic medium in the allure, which in turn results in dication formation. The two amino nitrogen in porphyrin core picks up two additional hydrogen ions and undergoes protonation which inturn induces positive charge in central core of porphyrin molecule thereby by increasing HOMO-LUMO energy gap. This decrease in no of Q bands to single sharp band is ascribed to increase of D_2h symmetry to D_4h by protonation and dication formation. Further extension of pronounced shoulder to B band which is very low in intensity at around ~365 (±5) nm present among all corresponding compounds is assigned to chare transfer transition from nonbonding lone pair P orbital of peripheral halogen atoms to empty π^* orbital of porphyrin. For bromo and iodo derivative the charge transfer could diversify from $n \rightarrow \pi^*$, $d \rightarrow \pi^*$, or $\pi \rightarrow d$ transitions at higher ionic strength [10]. Observation from spectral splitting and broadening of soret band suggesting aggregation character in acidic medium. In basic medium at pH= 10, the colour and absorption spectra remain marginally same as that of neutral environment. There was no any abrupt change in colour, it appears light pink, either the pattern of absorption spectra coincide with absorption spectra of pH= 7, with increasing intensity of soret and Q-bands. However the porphyrin core undergoes deprotonation and remains in dianionion form, leaving aside hyperpophyrin effect. From absorption spectral behaviour it can be clearly noticed that at higher pH values, absorption spectra show regular pattern as that of neutral environment indicting structural stability of porphyrin ring. Structure of H_2TXPP at various pH is represented in Fig. 4.

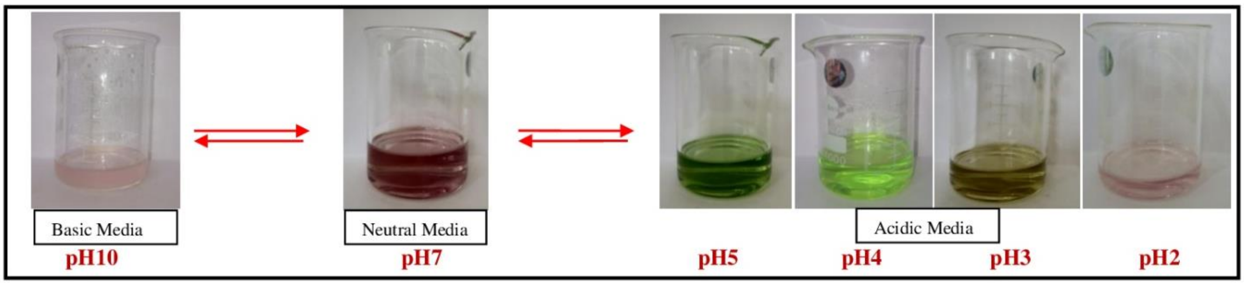

Fig. 3: Effect and change on colour of H_2TXPP analyate on pH variations.

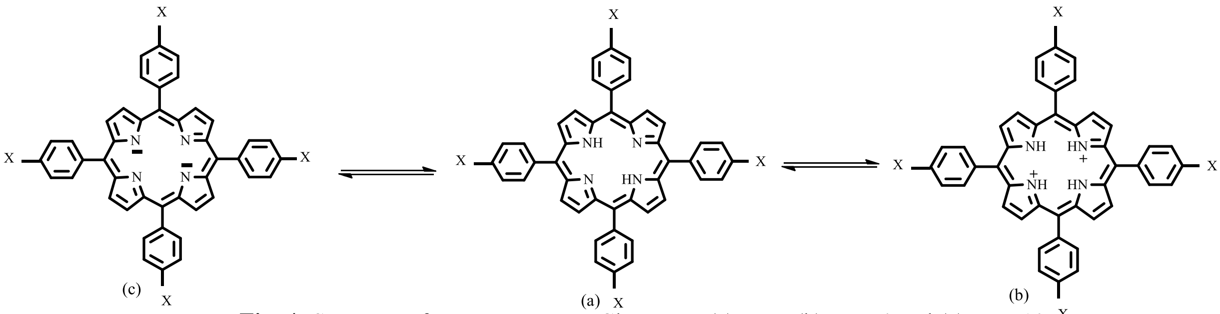

Fig. 4: Structure of H_2TXPP; X= F, Cl, Br, I at (a) pH7, (b) pH= 4 and (c) pH =10

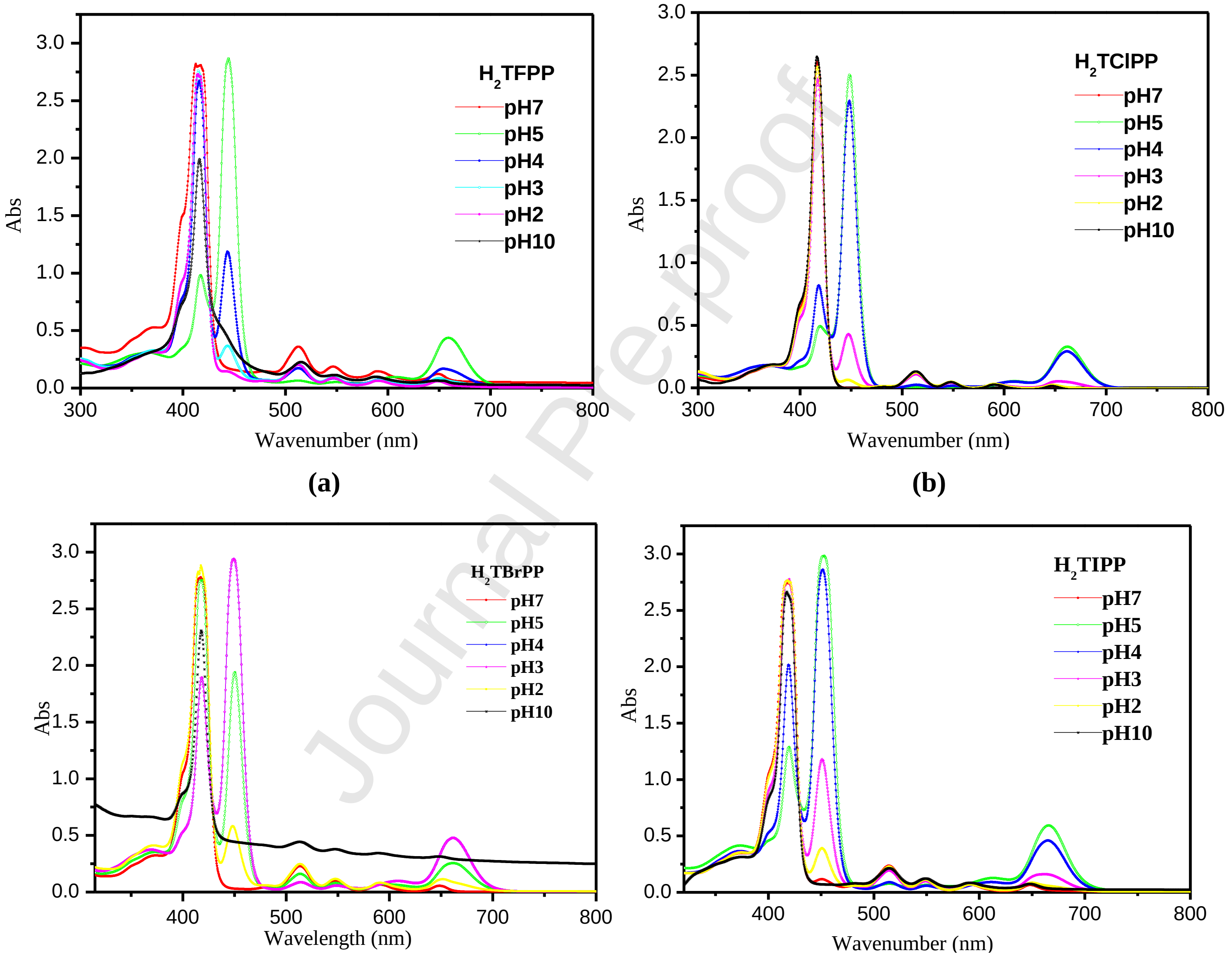

(a) **(b)**

(c) **(d)**

Fig. 5a: UV-Visible absorption spectra of H_2TXPP; (**a**) H_2TFPP, (**b**) H_2TClPP, (**c**) H_2TBrPP and (**d**) H_2TIPP at various pH scales in THF+H_2O system.

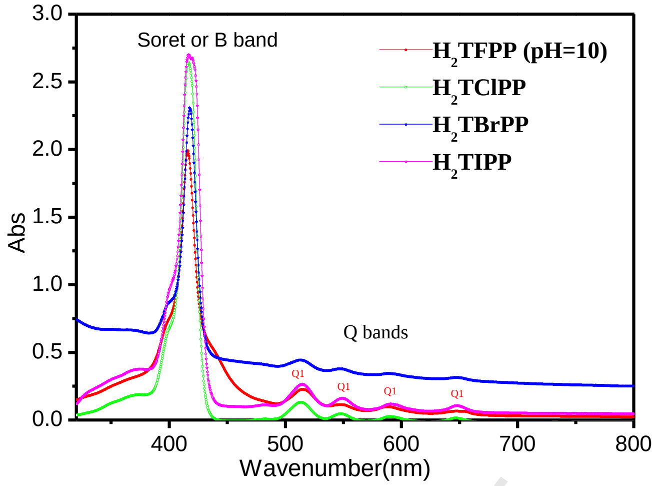

Fig. 5b: UV-Visible absorption spectra of H_2TXPP at pH= 10, in THF+H_2O system.

Emission Spectroscopy

Emission spectra of porphyrin i.e. H_2TXPP series was recorded at various pH ranges from acidic (pH=5-2), basic (pH=10) in THF+ H_2O medium at single concentration C_M= 3.0×10^{5}M with excitation wavelength 415 nm. The emission spectra for corresponding series are presented in Fig. (6a-6b). Featured characterises emission peaks of H_2TXPP series are presented in Table 4. All the spectra of corresponding series exhibit two potential bands. A high intensity band at around ~654 (±3) nm assigned to Q(0,0) and weak band at ~712 (±5) to Q(0,1) electronic transition. These two bands in visible region reflect usual S_1 emission. However the less common B(0,0) band in UV region appears at ~475 (±5) nm reflects S_2 emission. By continuously monitoring emission spectra induced by the exposure to acidic and basic media, we observed linearity and decreases in intensity with lowering pH values. However in basic medium the emission spectrum coincides with neutral medium, however there was decrease in intensity in the later. Previously reported fluorescence characterization and less common S_2-S_0 emission is parallel to our results and are in close relationship with absorption spectra [14,15,32]. It has been argued and reported that on absorption of UV-Visible radiation, π electrons of conjugated system undergoes excitation from (S_0) → (S_1 or S_2). Which in turn return to ground state in very short span of time and emit fluorescence at ~470 and 650-720 nm respectively. However the fluorescence quantum yields (Φ_f) depends on the peripheral phenyl functional groups. The values obtained are as (Φf = 0.052, 0.050, 0.054, 0.046 for F, Cl, Br and H_2TIPP). Heavier halogen atoms decrease the quantum yield with least for H_2TIPP.

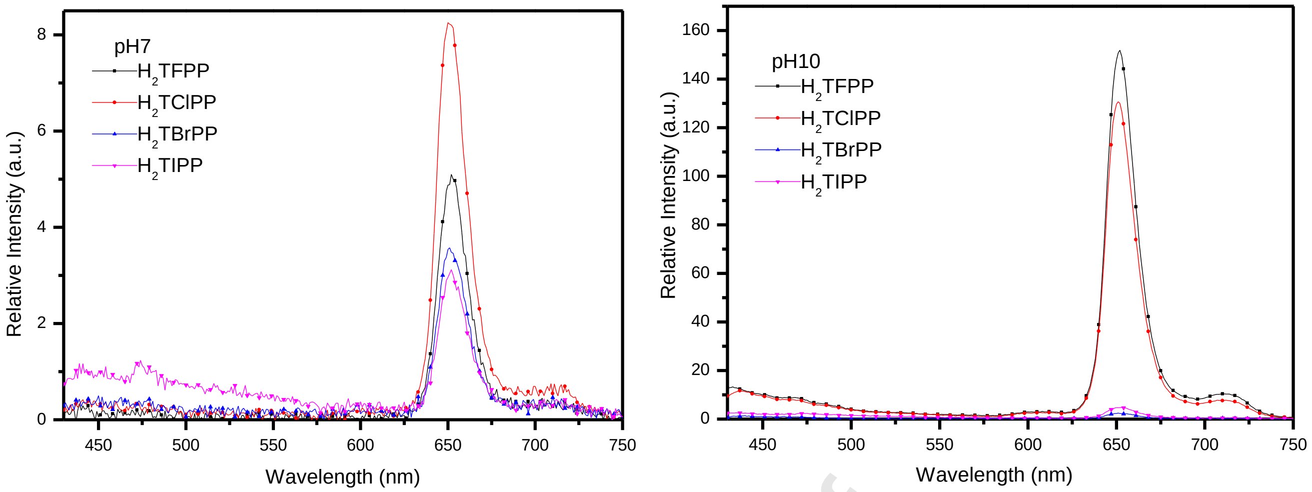

(a) **(b)**

Fig. 6(a): (**a**) Emission spectrum of H_2TXPP monomer in THF at pH=7 and (**b**) pH=10 (C_M = 3.0×10^5M)

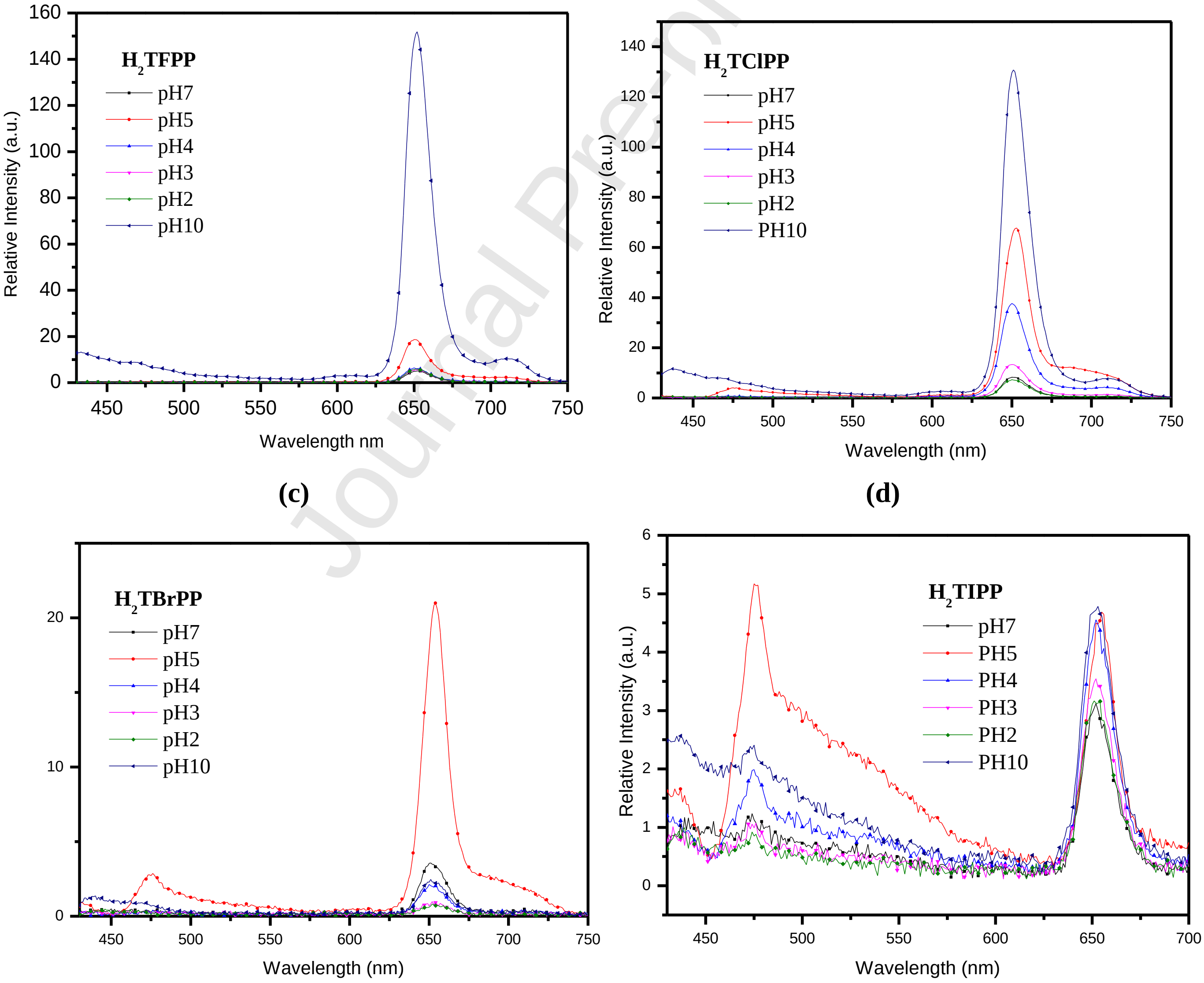

(c) **(d)**

(e) **(f)**

Fig. 6b: (c) Emission spectra of H_2TFPP, (**d**) H_2TClPP, (**e**) H_2TBrPP and (**f**) H_2TIPP at various pH scales in THF+H_2O system.

Table 4: Featured characterises emission peaks of H_2TXPP series

Compound	B(0,0)	Q(0,0)	Q(0,1)	Φf	Solvent	Ref.
TPP	-	654	712	0.110	DCM	[21,33]
H_2TFPP	470	652	712	0.052	$CHCl_3$	this work
H_2TClPP	475	651	711	0.050	$CHCl_3$	this work
H_2TBrPP	475	654/ 654	720/ 718	0.054	DCM/ $CHCl_3$	[34]/ this work
H_2TIPP	475	652	713	0.046	$CHCl_3$	this work

Aggregation behaviour

From the combined results from absorption and absorption-emission spectra for H_2TXPP series it is clearly evident that in pure organic solvents. The spectrum sows typical non aggregated monomeric complex. Indeed we measured the spectrum in THF and $CHCl_3$ solvent separately, the sharp absorption bands were observed in all the corresponding halo series indicating no aggregation of porphyrin. Further the absorption spectra in distinct organic solvent and at lowered concentrations show no any significant spectral changes. Upon introducing the pH variation in aqueous electrolyte solution, absorption spectra in acidic medium at around pH=4. Soret band splits into two individual lorentzains bands at ~444 (±10) and ~417 (±3) nm (known as j-band), accompanied by continuously broadening and red shift of soret band at 417 (±3) nm significant within all H_2TXPP series, which is attributed to side-by- side aggregation and formation of J-aggregate. The red shift of B band featured self aggregation through head-to-tail molecular ordering which is consonant with literature data [10,35]. The red shift observed is due to increased conjugation exerted by para substituted halogen group’s characteristic of electron donating tendency, which in turn reduces the HOMO-LUMO energy gap. Other spectral changes include reduction of Q bands to only single Q1 band, which is otherwise forbidden. The Q1 band is red shifted towards 647 (±5) nm with significant increase of the intensity. These changes in spectrum are attributed to increases of symmetry followed by dication formation at higher ionic strength. Absorption spectral pattern for electrically neutral and basic allure at pH=10 coincides, the modest differences consists only in enhancement of intensity of soret band. Indeed the hyperporphyrin effect is missing and exhibits dianionic form.

Conclusion

In conclusion, H_2TXPP series shows some variable electro-optic spectral changes on varying pH from acidic, basic and neutral medium in pure organic and aqueous electrolyte solution. UV-Visible and fluorescence spectroscopy were employed to study aggregation behaviour indeed.

Acknowdelegment

U.A.D is great full to NIT Srinagar for financial support in the form of research stipend and research facilities.

References

[1] E. Fagadar-Cosma, D. Vlascici, M. Birdeanu, G. Fagadar-Cosma, Novel fluorescent pH sensor based on 5-(4-carboxy-phenyl)-10,15,20-tris(phenyl)-porphyrin, Arab. J. Chem. 12 (2019) 1587–1594. https://doi.org/10.1016/j.arabjc.2014.10.011.

[2] M.M. Al Mogren, N.M. Ahmed, A.A. Hasanein, Molecular modeling and photovoltaic applications of porphyrin-based dyes: A review, J. Saudi Chem. Soc. 24 (2020) 303–320. https://doi.org/10.1016/j.jscs.2020.01.005.

[3] J. Chen, Y. Gao, Y. Xu, F. Xu, Q. Zhang, X. Lu, Theoretical study of novel porphyrin D-π-A conjugated organic dye sensitizer in solar cells, Mater. Chem. Phys. 225 (2019) 417–425. https://doi.org/10.1016/j.matchemphys.2018.12.105.

[4] S.C. Afonso, R. Enríquez De Salamanca, A.M. Del, The photodynamic and non-photodynamic actions of porphyrins, Brazilian J. Med. Biol. Res. 32 (1999) 255–266. https://doi.org/10.1590/S0100-879X1999000300002.

[5] M. Ethirajan, Y. Chen, P. Joshi, R.K. Pandey, The role of porphyrin chemistry in tumor imaging and photodynamic therapy, Chem. Soc. Rev. 40 (2011) 340–362. https://doi.org/10.1039/b915149b.

[6] T. Lee, X. an Zhang, S. Dhar, H. Faas, S.J. Lippard, A. Jasanoff, In Vivo Imaging with a Cell-Permeable Porphyrin-Based MRI Contrast Agent, Chem. Biol. 17 (2010) 665–673. https://doi.org/10.1016/j.chembiol.2010.05.009.

[7] J. Lu, S. Liu, M. Wang, Push-pull zinc porphyrins as light-harvesters for efficient dye-sensitized solar cells, Front. Chem. 6 (2018) 541. https://doi.org/10.3389/fchem.2018.00541.

[8] M.O. Senge, M. Fazekas, E.G.A. Notaras, W.J. Blau, M. Zawadzka, O.B. Locos,

E.M.N. Mhuircheartaigh, Nonlinear optical properties of porphyrins, Adv. Mater. 19 (2007) 2737–2774. https://doi.org/10.1002/adma.200601850.

[9] P. Dechan, G.D. Bajju, P. Sood, U.A. Dar, Crystallographic elucidations of indium(III) porphyrin conformations, morphology and aggregation behaviour: Comparative optical study of free base porphyrins and their indium(III) derivatives at varying pH, J. Mol. Struct. 1183 (2019) 87–99. https://doi.org/10.1016/J.MOLSTRUC.2019.01.064.

[10] P. Dechan, G.D. Bajju, P. Sood, U.A. Dar, Synthesis and single crystal structure of a new polymorph of 5, 10, 15, 20-tetrakis-(4-chlorophenyl) porphyrin, H_2TTPCl_4 : Spectroscopic investigation of aggregation of H_2TTPCl_4, Mol. Cryst. Liq. Cryst. 666 (2018) 79–93. https://doi.org/10.1080/15421406.2018.1512546.

[11] N. Amiri, M. Hajji, T. Roisnel, G. Simonneaux, H. Nasri, Synthesis, molecular structure, photophysical properties and spectroscopic characterization of new 1D-magnesium(II) porphyrin-based coordination polymer, Res. Chem. Intermed. 44 (2018) 5583–5595. https://doi.org/10.1007/s11164-018-3442-9.

[12] A.R. Da Silva, A.C. Pelegrino, A.C. Tedesco, R.A. Jorge, Photodynamic activity of chloro(5,10,15,20-tetraphenylporphyrinato) indium(III), J. Braz. Chem. Soc. 19 (2008) 491–501. https://doi.org/10.1590/s0103-50532008000300017.

[13] N. Amiri, S. Nouir, M. Hajji, T. Roisnel, T. Guerfel, G. Simonneaux, H. Nasri, Synthesis, structure, photophysical properties and biological activity of a cobalt(II) coordination complex with 4,4′-bipyridine and porphyrin chelating ligands, J. Saudi Chem. Soc. (2019). https://doi.org/10.1016/j.jscs.2019.03.003.

[14] E. Fagadar-Cosma, D. Vlascici, M. Birdeanu, G. Fagadar-Cosma, Novel fluorescent pH sensor based on 5-(4-carboxy-phenyl)-10,15,20-tris(phenyl)-porphyrin, Arab. J. Chem. 12 (2019) 1587–1594. https://doi.org/10.1016/j.arabjc.2014.10.011.

[15] E. Fagadar-Cosma, C. Enache, R. Tudose, I. Armeanu, E. Mosoarca, D. Vlascici, O. Costisor, UV-VIS and fluorescence spectra of meso-tetraphenylporphyrin and meso-tetrakis-(4-methoxyphenyl) porphyrin in THF and THF-water systems. The influence of pH, Rev. Chim. 58 (2007) 451–455.

[16] M. Plaschke, R. Czolk, H.J. Ache, Fluorimetric determination of mercury with a water-soluble porphyrin and porphyrin-doped sol-gel films, Anal. Chim. Acta. 304 (1995) 107–113. https://doi.org/10.1016/0003-2670(94)00568-7.

[17] D. Tatman, P.A. Liddell, T.A. Mooret, D. Gustt, A.L. Mooret, Carotenohematoporphyrins as Tumor-Imaging Dyes . Synthesis and ln Vifro Photophysica I Characterization *, 68 (1998) 459–466.

[18] M. La Penna, M.G. Alvarez, E.I. Yslas, V. Rivarola, E.N. Durantini, Characterization of photodynamic effects of meso-tetrakis-(4-methoxyphenyl) porphyrin: Biological consequences in a human carcinoma cell line, Dye. Pigment. 49 (2001) 75–82. https://doi.org/10.1016/S0143-7208(01)00010-9.

[19] J.P. Keene, D. Kessel, E.J. Land, R.W. Redmond, T.G. Truscott, DIRECT DETECTION OF SINGLET OXYGEN SENSITIZED BY HAEMATOPORPHYRIN AND RELATED COMPOUNDS, Photochem. Photobiol. 43 (1986) 117–120. https://doi.org/10.1111/j.1751-1097.1986.tb09501.x.

[20] J.M. Wessels, W. Strauß, H.K. Seidlitz, A. Rück, H. Schneckenburger, Intracellular localization of meso-tetraphenylporphine tetrasulphonate probed by time-resolved and microscopic fluorescence spectroscopy, J. Photochem. Photobiol. B Biol. 12 (1992) 275–284. https://doi.org/10.1016/1011-1344(92)85029-T.

[21] G.A. Crosby, J.N. Demas, Measurement of photoluminescence quantum yields. Review, J. Phys. Chem. 75 (1971) 991–1024. https://doi.org/10.1021/j100678a001.

[22] A.D. Adleb, F.R. Longo, J.D. Finarelli, J. Goldmacher, J. Assour, L. Korsakoff, A Simplified Synthesis for Meso-Tetraphenylporphine, J. Org. Chem. 32 (1967) 476. https://doi.org/10.1021/jo01288a053.

[23] B.M.L. Chen, A. Tulinsky, Redetermination of the Structure of Porphine, J. Am. Chem. Soc. 94 (1972) 4144–4151. https://doi.org/10.1021/ja00767a015.

[24] L.E. Webb, E.B. Fleischer, Crystal structure of porphine, J. Chem. Phys. 43 (1965) 3100–3111. https://doi.org/10.1063/1.1697283.

[25] T. Hökelek, D. Ülkü, N. Gündüz, M. Hayvali, Z. Kiliç, IUCr, 5,10,15,20-Tetrakis(p-chlorophenyl)porphyrin, Acta Crystallogr. Sect. C Cryst. Struct. Commun. 49 (1993) 1667–1670. https://doi.org/10.1107/S0108270193000782.

[26] N. Amiri, M. Hajji, F. Ben Taheur, S. Chevreux, T. Roisnel, G. Lemercier, H. Nasri, Two novel magnesium(II) meso-tetraphenylporphyrin-based coordination complexes: Syntheses, combined experimental and theoretical structures elucidation, spectroscopy, photophysical properties and antibacterial activity, J. Solid State Chem. 258 (2018) 477–484. https://doi.org/10.1016/j.jssc.2017.11.018.

[27] H. Yaman, A. Kayan, Synthesis of novel single site tin porphyrin complexes and the catalytic activity of tin tetrakis(4-fluorophenyl)porphyrin over -caprolactone, J. Porphyr. Phthalocyanines. 21 (2017) 231–237. https://doi.org/10.1142/S1088424617500407.

[28] P. Bhyrappa, K.S. Suslick, Synthesis and Crystal Structure of 5,10,15,20-Tetrakis(3,5-

dinitrophenyl)porphyrin †, n.d. http://suslick.scs.illinois.edu/documents/jporphphthal98391.pdf (accessed July 16, 2019).

[29] J.B. Kim, J.J. Leonard, F.R. Longo, Mechanistic study of the synthesis and spectral properties of meso-tetraarylporphyrins, J. Am. Chem. Soc. 94 (1972) 3986–3992. https://doi.org/10.1021/ja00766a056.

[30] H. Guo, J. Jiang, Y. Shi, Y. Wang, Y. Wang, S. Dong, Sequential deprotonation of meso-(p-hydroxyphenyl)porphyrins in DMF: From hyperporphyrins to sodium porphyrin complexes, J. Phys. Chem. B. 110 (2006) 587–594. https://doi.org/10.1021/jp0523827.

[31] D. Khusnutdinova, M. Flores, A.M. Beiler, G.F. Moore, Synthesis and characterization of a cobalt(II) tetrakis(3-fluorophenyl) porphyrin with a built-in 4-vinylphenyl surface attachment moiety, Photosynthetica. (2018). https://doi.org/10.1007/s11099-018-0783-y.

[32] D.L. Akins, S. Özçelik, H.R. Zhu, C. Guo, Fluorescence decay kinetics and structure of aggregated tetrakis(p-sulfonatophenyl)porphyrin, J. Phys. Chem. 100 (1996) 14390–14396. https://doi.org/10.1021/jp961013v.

[33] O. Nicrosini, L. Trentadue, Soft photons and second order radiative corrections to e+e-→Z0, Phys. Lett. B. 196 (1987) 551–556. https://doi.org/10.1016/0370-2693(87)90819-7.

[34] N. Amiri, F. Ben Taheur, S. Chevreux, E. Wenger, G. Lemercier, H. Nasri, Synthesis, crystal structure and spectroscopic characterizations of porphyrin-based Mg(II) complexes – Potential application as antibacterial agent, Tetrahedron. 73 (2017) 7011–7016. https://doi.org/10.1016/j.tet.2017.10.029.

[35] A. Eisfeld, J.S. Briggs, The J- and H-bands of organic dye aggregates, Chem. Phys. 324 (2006) 376–384. https://doi.org/10.1016/j.chemphys.2005.11.015.

Graphical Abstract

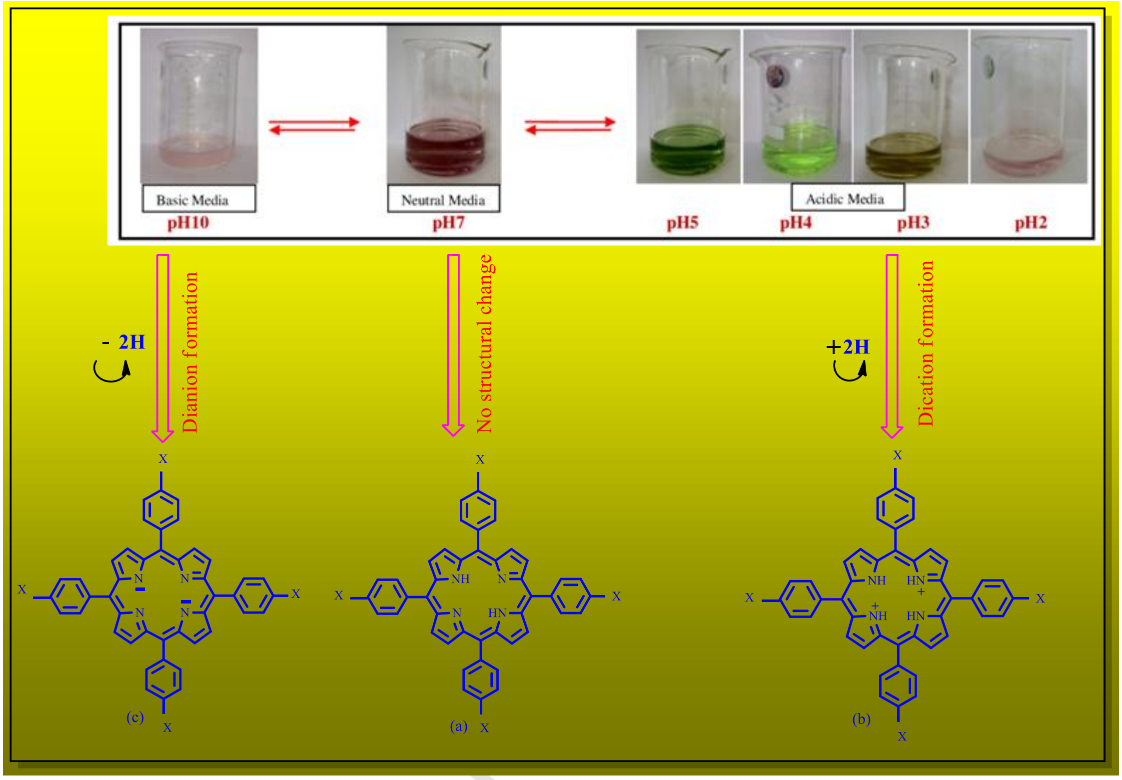

Highlights

- Optical and fluorescence response of halogen derivatives of meso-tetrakis-(4-phenyl) porphyrin; TPP.
- Effect on absorption and emission spectrum of meso-tetrakis-(4-halophenyl) porphyrin; H_2TXPP on pH variation.
- Specific structural changes and aggregation behavior.